Appl Phys A (2008) 93: 745–749
DOI 10.1007/s00339-008-4706-9

Applied Physics A
Materials Science & Processing

Synthesis of DLC films by PLD from liquid target and dependence of film properties on the synthesis conditions

Jaanus Eskusson · Raivo Jaaniso · Enn Lust

Received: 12 October 2007 / Accepted: 4 March 2008 / Published online: 17 June 2008

Abstract DLC (Diamond-like carbon films) were prepared by pulsed laser ablation of a liquid target at substrate temperatures from 18 to 600°C using 248 nm KrF excimer laser. The sp^3 hybridization state carbon formation was additionally promoted by gaseous H_2O_2 flow through the reaction chamber and substrate excitation by the same laser beam.

Deposited DLC films were characterised by Raman scattering spectroscopy and atomic force microscopy (AFM). Comparative AFM and Raman study shows that the increase in the content of sp^3 type bonding in DLC is in correlation with the increase of the surface roughness of the samples prepared.

PACS 07.30.-t · 68.60.Bs · 81.05.Uw

1 Introduction

Experimental evidence suggests that usually over 80% of the atoms in amorphous carbon (a-C) thin films are in the sp^2 hybridization state [1]. Interest in a-C is due to its thermal stability and diamond-like tribological properties [2, 3]. DLC films, also known as tetrahedral a-C films, usually contain a relatively high proportion of sp^3 hybridised carbon atoms together with sp^2 hybridised carbon bonds. The complex bonding structure results in a unique combination of DLC properties. Thin films of this material exhibit a wide range of mechanical, electronic, electro-chemical and antimicrobial properties. They are very suitable for protective coatings, optical devices, field emission components, coatings for biocompatible implants and other medical devices [4–12].

PLD (pulsed laser deposition) has proved to be an effective technique for deposition of a wide variety of thin film materials, including DLC [13–15]. The PLD process is popular for its ability to generate very active intermediate carbon species, which enhances the formation of a high percentage of sp^3 bonded carbon atoms in DLCs.

The ratio of sp^3/sp^2 carbon atoms in diamond-like films depend on process parameters such as type and pressure of the reagent gas, substrate temperature, laser wavelength and power density [16].

2 Experimental

The scheme of the PLD system setup for DLC thin film synthesis is shown in Fig. 1. All depositions were carried out at temperatures from 18 to 600°C and pressures from 4×10^{-7} to 2×10^{-3} bar. The DLC film deposition equipment was composed of a KrF eximer laser (ESTLA EXC-150/25) which produced 25 ns pulses with a maximum energy of 250 mJ; a laser beam intensity regulating system; a computer controlling the laser beam intensity regulating system and the laser itself; optical components; a pumping system with valves; a reaction chamber; and a H_2O_2 reservoir.

A vacuum oil Santovac-5 [17, 18] was used as the ablation source (target). This oil has a very low vapor pressure ($P^{20°C} = 2.6 \times 10^{-10}$ mbar) and a very high absorption coefficient at our laser wavelength, 248 nm. Taking into account our future goal—synthesis of DLC films doped with

J. Eskusson (✉) · E. Lust
Institute of Chemistry, University of Tartu, Jakobi 2, Tartu, 51014 Estonia
e-mail: jaanus.eskusson@ut.ee

R. Jaaniso
Institute of Physics, University of Tartu, Riia 142, Tartu, 51014 Estonia

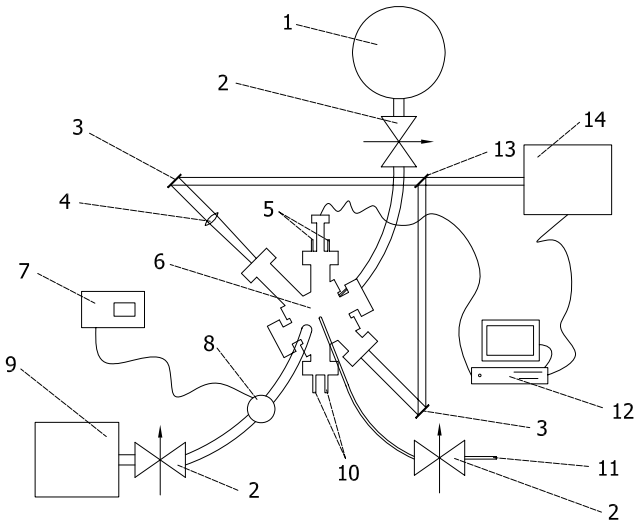

Fig. 1 Schematic representation of DLC films synthesis. *1*—He cryogenic pump, *2*—valve, *3*—mirror, *4*—lens, *5*—heater and thermocouple connection, *6*—deposition chamber, *7*—controller, *8*—vacuum gauge, *9*—vacuum pump, *10*—target cooling tubes, *11*—reagent gas (H_2O_2) inlet, *12*—PC, *13*—semitransparent mirror, *14*—excimer laser (248 nm)

rare earth metal cations—the liquid target under discussion is more suitable for preparation of metal-organic complex solution in Santovac. On the other hand, the absence of the target moving system simplifies the deposition chamber noticeably.

In our experiment Santovac-5 (1 mm thick layer) is situated at the bottom of the cooling target holder and was previously vacuumed from dissolved gases. The distance between the target and the substrate was 4 cm. Fused silica plates (1 × 10 × 10 mm) were used as substrates which were cleaned firstly mechanically thereafter cleaned for 10 minutes in a sonic bath with acetone and after that rinsed with ethanol and methanol.

The deposition chamber has three connection tubes (Fig. 1): one tube connects the chamber with the He cryogenic pump; the second tube, opposite the first tube, connects the chamber with an H_2O_2 reservoir, and the third tube is for the pre-vacuum pump. The connection of the pre-vacuum pump was closed before the beginning of the deposition process, and the cryogenic pump during the deposition process was used. Through the valve between the H_2O_2 reservoir and the deposition chamber we can control the amount of H_2O_2 vapor flowing into the deposition chamber. It should be noted that in the literature there is no detailed mechanism explaining the influence of H_2O_2 vapor on the sp^3 hybridised carbon formation process; however, there are some experimental reports demonstrating the influence of H_2O_2 vapor on the DLC film formation process [19]. The level of base vacuum before the reagent gas valve was opened was up to 10^{-6} mbar.

Before entering into the deposition chamber the applied laser beam has been divided by the semitransparent (50%) mirror into the two parts (Fig. 1). One part of the divided laser beam was focused by the quarts lens on the liquid target with a spot size of ∼1.5 mm^2 and the second nonfocused laser beam irradiated at same time the crowing DLC film on the silica substrate. Based on our previous experimental studies [20] where the noticeable influence of the laser irradiation on the content of carbon in sp^3 hybridization state in DLC films has been demonstrated, we assume that the laser activation is very useful for the DLC formation process. The laser pulse frequency was all the time 10 Hz and the laser beam intensity varied from 20 to 130 mJ of energy (1.3–8.7 J/cm^2) per impulse to the ablation target.

The DLC films prepared were characterised by Raman scattering spectroscopy and AFM. Raman spectra were recorded by a double diffraction lattice spectrometer (SPEX 1402). The excitation light source was an Ar laser with 488 nm wavelength and the detection unit was a CCD camera. Film surface microstructure analyses were performed by an AFM (Autoprobe CP) in contact mode regime. All DLC film characterisations were made at room temperature.

3 Results and discussion

3.1 Raman spectroscopy of the films

It should be noted that different interpretations of the Raman spectra for amorphous carbon film structures and corresponding structural changes were discussed in literature [21–26].

We studied the prepared DLC films, using Raman spectra shape dependences from the deposition parameters and compared these spectra with the DLC spectra given in the literature. The main interesting deposition parameters were laser beam intensity, the amount pressure of H_2O_2 vapour in the deposition chamber and the substrate temperature.

In this study a major influence of laser beam intensity appeared on the G band position in the Raman spectra for the DLC films. It is probable that when the laser beam intensity is increased it can induce bigger sp^2 hybridised carbon bonds deformation and partial transformation to the sp^3 hybridization state; this was confirmed by the Raman spectra G band moving to shorter wavenumbers in Fig. 2.

The Raman spectra in Fig. 2 characterise DLC films of which the only difference in deposition conditions was the laser beam intensity, and this is the main reason why G band shifts occur from 1573 cm^{-1} (a) to 1580 cm^{-1} (b) in the Raman spectra for the DLC film.

The influence of H_2O_2 vapour on the DLC films structure was estimated using the Raman spectra given in Fig. 3,

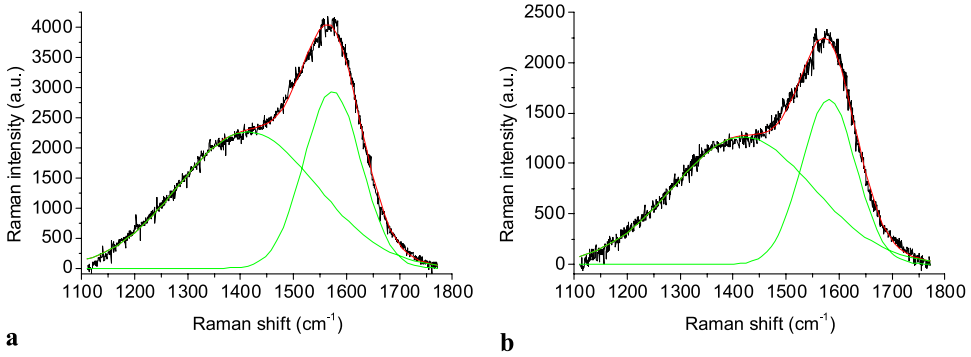

Fig. 2 Raman spectra of the DLC films, deposited using 35 mJ (**a**) and 25 mJ laser beam intensity (**b**). Both films were deposited at 500°C substrate temperature using 3000 laser impulses in 9×10^{-3} mbar H_2O_2 vapor pressure. Both film were deposited using additional film excitation by the laser beam irradiation

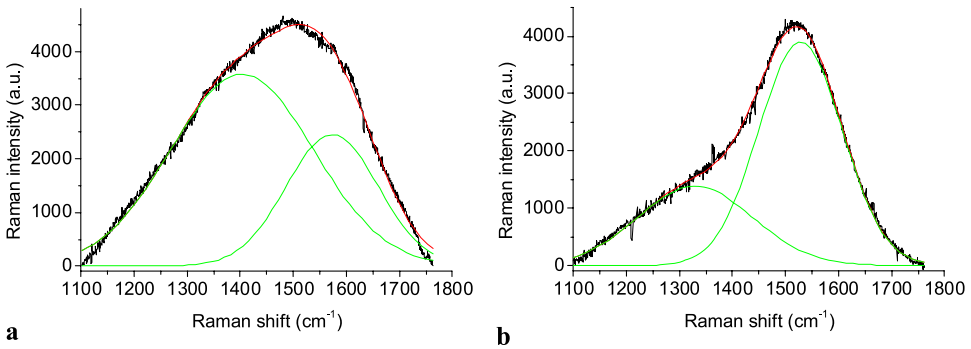

Fig. 3 Raman spectra of the DLC films deposited in 1.9 mbar (**a**) and 2.7×10^{-3} mbar H_2O_2 vapor pressure (**b**). Both films were deposited at 22°C substrate temperature using 5000 laser impulses with 130 mJ laser beam intensity (without additional laser activation of the surface layer)

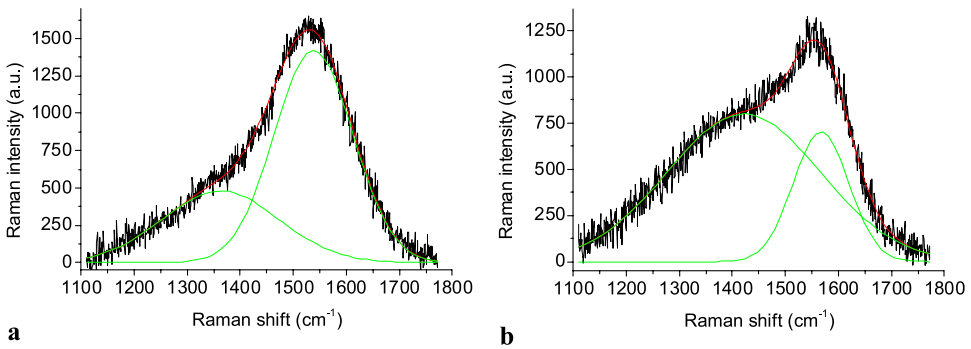

Fig. 4 Raman spectra of the DLC films deposited at 100°C (**a**) and 600°C (**b**) substrate temperature. Both films were deposited using 35 mJ laser beam intensity and 9×10^{-3} mbar H_2O_2 vapor pressure. During deposition, the surfaces were additionally irradiated by the laser beam. The number of laser impulses for (**a**) and (**b**) is 3000 and 2000, respectively

where the H_2O_2 vapour concentration was varied during the deposition process.

We can see in Fig. 3a that the ratio of Raman intensities I_D/I_G (2.26) is much higher than in Fig. 3b (0.48). An increase of the D band intensity compared with the G band intensity and its frequency shift to higher frequencies means that in this film the number of ordered aromatic carbon rings increases with decreasing size of aromatic clusters [27]. Very similar Raman spectra were published in the literature [24, 25, 28–31], where ∼80% sp^3 hybridised carbon content was calculated based on the EELS data [32].

It was established that at higher substrate temperatures the G band in the Raman spectra shifts toward higher frequencies, as given in Fig. 4. In this figure we can see two different shapes of Raman spectra for DLC films deposited at different conditions. It was established that the DLC film structure depends mainly on the substrate temperature and the number of laser impulse does not have a great influence on the film structure (change is mainly in the film thickness).

Observed G band shift to higher wavenumbers ($1538\,cm^{-1} \rightarrow 1567\,cm^{-1}$) at higher substrate temperatures can be explained by the excitation of carbon particles on the substrate surface so that they achieve the ability to overrun the activation energy barrier between the sp^3 and sp^2 hybridised carbon state. Such an equilibrium of an energetic overrun promotes, preferably, a lower energetic state, which in this case, is the graphitic structure. The graphitic structure, characterised by shorter bonds compared to average DLC bonds and therefore larger oscillation frequencies, which appear in the G band shifting to the higher wavenumbers in the Raman spectra, are typical.

Using the Raman spectra of several DLC films grown at different substrate temperatures, a linear dependence be-

tween the substrate temperature and G band scattering maximum position was observed, as given in Fig. 5.

3.2 Atomic force microscopy of the films

AFM measurements were performed in the contact mode regime and results obtained indicate that the most important influence in the deposition process for the DLC films surface structure was the substrate temperature. The main surface structure representing a characterizing parameter is the root-mean-square (RMS) roughness:

$$\mathrm{RMS} = \sqrt{\frac{\sum_{n=1}^{N}(Z_n - \overline{Z})^2}{N-1}},$$

N is a number of data points and $\overline{Z}$ is the average height.

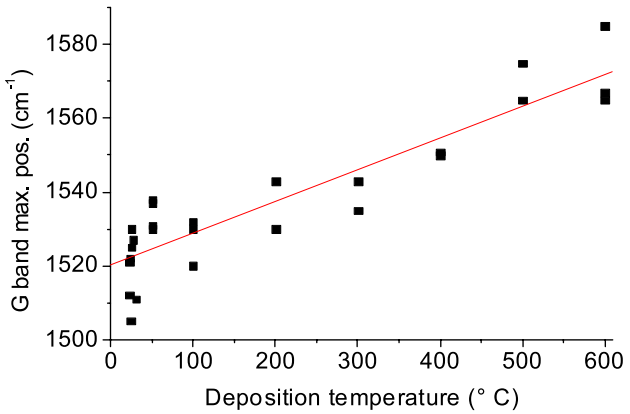

Fig. 5 DLC films Raman spectra G band maximum position dependence on substrate temperature

In Fig. 6 the RMS roughness dependences on the DLC films growing substrate temperature (other deposition parameters were similar) are given.

According to these data it was established that a noticeable RMS roughness change occurs at temperatures between 50 and 100°C. At higher temperatures the RMS rougness values approach a plateau. 3D images of DLC films surface profiles deposited at different temperatures can be seen in Fig. 7. The two upper AFM images in Fig. 7 have been made from the DLC film which was deposited at 25°C substrate temperature (40 mJ laser beam intensity, 9.7×10^{-3} mbar H_2O_2 vapor pressure and 3500 laser impulses). The two lower AFM images were made from DLC films deposited

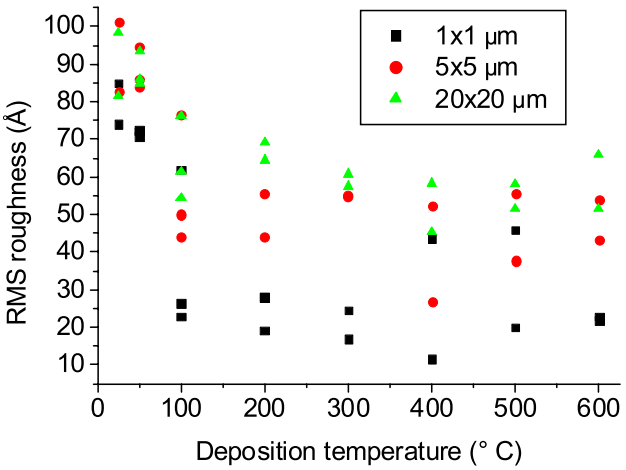

Fig. 6 DLC films RMS, substrate temperature dependences established for the 1×1 µm, 5×5 µm and 20×20 µm films areas

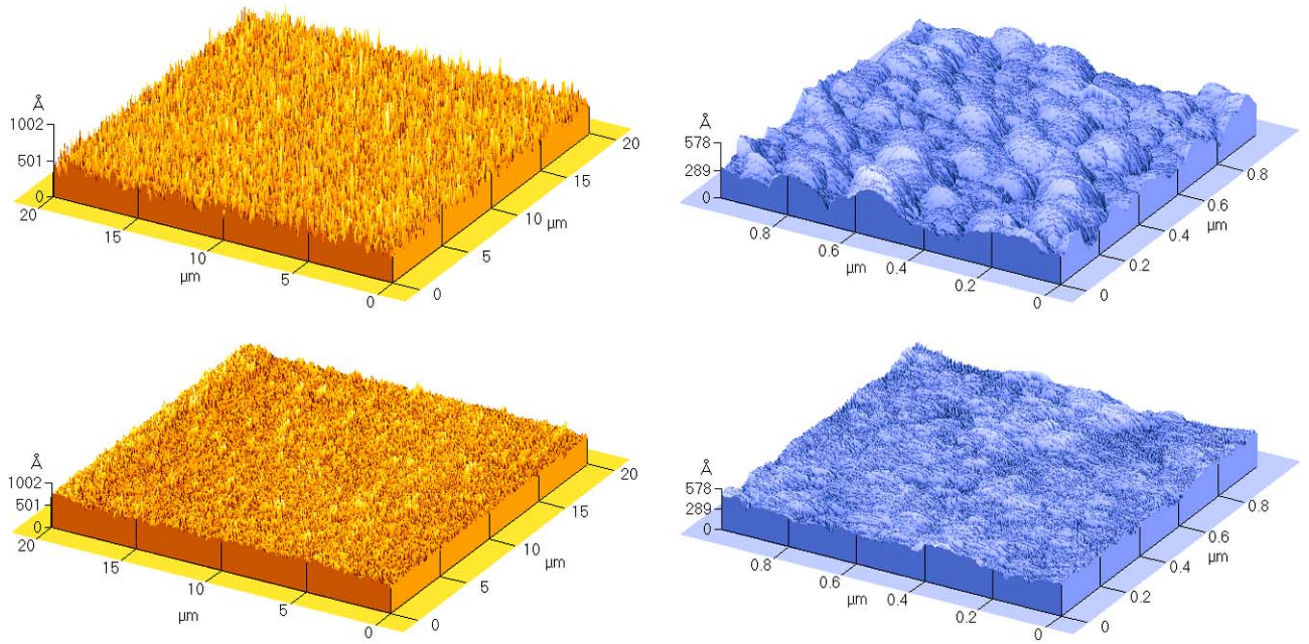

Fig. 7 AFM 3D images from DLC films where *upper areas* were deposited at 25°C and *lower areas* were deposited at 400°C

at 400°C substrate temperature (35 mJ laser beam intensity, 9.5×10^{-3} mbar H_2O_2 vapor pressure and 3000 laser impulses). In both experiments the laser beam excitation method was used.

Figure 7 demonstrates that at a lower deposition temperature, the larger grain size surface structure (grain size: 50–150 nm), and a smoother surface profile at higher deposition temperatures was grown. The RMS roughness of these films is 74 Å and 44 Å on a 1×1 μm surface area and 82 Å and 58 Å on a 20×20 μm surface area, respectively.

According to the literature there are discrepant tendencies discussed in the influence of the deposition temperature on the RMS roughness values for the DLCs. It should be noted that based on results of [33], a noticeable cluster formation at higher deposition temperatures is possible and using the AFM data corresponding to measurements with a larger surface area than the size of the clusters, RMS values increase drastically.

4 Conclusion

The influence of the deposition parameters on the DLC film properties has been studied. The influence of the laser beam intensity, the pressure of the H_2O_2 vapour in the deposition chamber and the substrate temperature on the DLC has been analysed.

The results obtained indicate that a higher laser beam intensity used for the ablated material enhanced the formation of sp^3 hybridised carbon content in the DLC films.

With increasing H_2O_2 vapour pressure in the deposition chamber the number of ordered aromatic carbon rings increases with decreasing size of the aromatic clusters in the DLC film structures.

A great influence of the substrate temperature on the DLC structure has been established. The results of Raman studies indicated that at higher substrate temperatures the G band shifts toward to higher frequencies which demonstrates preferable sp^3 hybridised carbon transformation to the sp^2 hybridised carbon structure. The dependence of the G band Raman shift on the substrate temperature was quite linear. AFM studies indicated that lower deposition temperatures resulted in bigger grain sizes of the film surface structures. A sudden drop in the RMS values has been observed in a relatively narrow range of temperature (50–100°C), whereas at higher temperatures than 100°C the RMS value changed relatively slowly.

References

1. D.R. McKenzie, D. Muller, B.A. Pailthorpe, Phys. Rev. Lett. **67**, 773 (1990)
2. A.A. Voevodin, M.S. Donley, J.S. Zabinsky, J.E. Bultman, Surf. Coat. Technol. **77**, 534 (1995)
3. M.P. Siegal, D.R. Tallant, P.N. Provencio, D.L. Overmyer, R.L. Simpson, Appl. Phys. Let. **76**, 3052 (2000)
4. A. Grill, V. Patel, Diamond Relat. Mater. **2**, 597 (1993)
5. A. Matthews, S.S. Eskildsen, Diamond Relat. Mater. **3**, 902 (1994)
6. A.A. Voevodin, M.S. Donley, Surf. Coat. Technol. **82**, 199 (1996)
7. J. Robertson, Mater. Sci. Eng. R Rep. **37**, 129 (2002)
8. A.M. Wu, J. Sun, X.K. Shen, N. Xu, Z.F. Ying, Z.B. Dong, J.D. Wu, Diamond Relat. Mater. **15**, 1235 (2006)
9. J. Robertson, Prog. Solid State Chem. **21**, 199 (1991)
10. Y. Lifshitz, Diamond Relat. Mater. **5**, 388 (1996)
11. A. Hu, I. Alkhesho, H. Zhou, W.W. Duley, Diamond Relat. Mater. **16**, 149 (2007)
12. M.L. Morrison, R.A. Buchanan, P.K. Liaw, C.J. Berry, R.L. Brigmon, L. Riester, H. Abernathy, C. Jin, R.J. Narayan, Diamond Relat. Mater. **15**, 138 (2006)
13. S.M. Mominuzzaman, T. Soga, T. Jimbo, M. Umeno, Thin Solid Films **376**, 1 (2000)
14. N. Benchikh, F. Garrelie, C. Donnet, K. Wolski, R.Y. Fillit, F. Rogemond, J.L. Subtil, J.N. Rouzaud, J.Y. Laval, Surf. Coat. Technol. **200**, 6272 (2006)
15. J.M. Lackner, C. Stotter, W. Waldhauser, R. Ebner, W. Lenz, M. Beutl, Surf. Coat. Technol. **174–175**, 402 (2003)
16. P.M. Ossi, C.E. Bottani, A. Miotello, Thin Solid Films **482**, 2 (2005)
17. Edwards: Vacuum products catalogue (1996–1997), p. 239 (1995)
18. R.-F. Xiao, Appl. Phys. Lett. **67**(7), 1022 (1995)
19. R.-F. Xiao, Appl. Phys. Lett. **67**(21), 3117 (1995)
20. J. Eskusson, R. Jaaniso, T. Avarmaa, T. Jantson, E. Lust, SPIE Proc. **6591**, 65910L/1 (2007)
21. D.S. Knigth, W.B. White, J. Mater. Res. **4**(2), 358 (1989)
22. R. Diamant, E. Jimenez, E. Haro-Poniatowski, L. Ponce, M. Fernandez-Guasti, J.C. Alonso, Diamond Relat. Mater. **8**, 1277 (1999)
23. V.N. Apakina, A.L. Karuzskii, M.S. Kogan, A.V. Kvit, N.N. Melnik, Yu.A. Mityagin, V.N. Murzin, A.A. Orlikovsky, A.V. Perestoronin, S.D. Tkachenko, N.A. Volchkov, Diamond Relat. Mater. **6**, 564 (1997)
24. D.R. Tallant, J.E. Parmeter, M.P. Siegal, R.L. Simpson, Diamond Relat. Mater. **4**, 191 (1995)
25. D.T. Peeler, P.T. Murray, Diamond Relat. Mater. **3**, 1124 (1994) (1994)
26. J.D. Carey, S.R.P. Silva, Phys. Rev. B **70**, 235417 (2004)
27. A.C. Ferrari, J. Robertson, Phys. Rev. B **61**(20), 14095 (2000)
28. M.L. Terranova, V. Sessa, S. Piccirillo, Appl. Phys. Lett. **75**(3), 379 (1999)
29. S. Leppävuori, J. Levoska, J. Vaara, O. Kusmartseva, Mater. Res. Soc. Symp. Proc. **285**, 557 (1993)
30. S.E. Johnson, M.N.R. Ashfold, M.P. Knapper, R.J. Lade, K.N. Rosser, N.A. Fox, W.N. Wang, Diamond Relat. Mater. **6**, 569 (1997)
31. M. Chhowalla, A.C. Ferrari, J. Robertson, G.A.J. Amaratunga, Appl. Phys. Lett. **76**(11), 1419 (2000)
32. Y. Lifshitz, G.D. Lempert, E. Grossman, I. Avigal, C. Uzan Saguy, R. Kalish, J. Kulik, D. Marton, J.W. Rabalais, Diamond Relat. Mater. **4**, 318 (1995)
33. E. Cappelli, C. Scilletta, S. Orlando, R. Flammini, S. Iacobucci, P. Ascarelli, Thin Solid Films **482**, 305 (2005)